Sensors and Materials, Vol. 37, No. 5 (2025) 1977–1991
MYU Tokyo

S & M 4035

Reduction of γ-ray-induced Noise of Diamond Detector Elements and Estimation of Neutron Detection Efficiency for the Development of a Criticality Proximity Monitoring System for the Decommissioning of the Fukushima Daiichi Nuclear Power Plant

Kengo Oda,[1*] Junichi H. Kaneko,[1] Yusuke Kobayakawa,[1] Kenichi Watanabe,[2] Youichi Fujita,[3] Eitaro Hamada,[3] Tetsuichi Kishishita,[3] Masaya Miyahara,[3] Masayoshi Shoji,[3] Hironori Uchinoyae,[3] Sho Nishino,[4] Yoshihiko Tanimura,[4] Akiyoshi Chayahara,[5] Takehiro Shimaoka,[5] Hideaki Yamada,[5] Tomohiro Endo,[6] Yuto Akashi,[1] and Manobu M. Tanaka[3]

[1]Hokkaido University, Kita 13 Nishi 8, Kita-ku, Sapporo, Hokkaido 060-8628, Japan
[2]Kyushu University, 744 Motooka, Nishi-ku, Fukuoka 819-0395, Japan
[3]High Energy Accelerator Research Organization, 1-1 Oho, Tsukuba, Ibaraki 305-0801, Japan
[4]Japan Atomic Energy Agency 2-4 Shirakata, Tokai-mura, Naka-gun, Ibaraki 319-1195, Japan
[5]National Institute of Advanced Industrial Science and Technology,
1-8-31 Midorigaoka, Ikeda, Osaka 563-8577, Japan
[6]Nagoya University, Furo-cho, Chikusa-ku, Nagoya, Aichi 464-8603, Japan

(Received February 7, 2025; accepted April 3, 2025)

Keywords: Fukushima Daiichi Nuclear Power Plant Decommissioning Project, criticality proximity monitoring system, diamond detection element, measurement circuit, γ-ray irradiation

In this paper, we discuss the development of a diamond detector element for a criticality proximity monitoring system, which is essential for the decommissioning of the Fukushima Daiichi Nuclear Power Plant. The system must withstand γ-rays at a dose rate of 1 kGy/h with minimal shielding due to payload constraints. We evaluated the effects of γ-rays on prototype diamond detectors and confirmed that removing the lift-off separation surface of diamond membrane by ion beam etching and adding a p+ diamond layer effectively reduced the effect of γ-rays. A prototype detector combined a 180-μm-thick ^{6}LiF sintered neutron-to-charged-particle converter with a diamond detector having a 2.53 mm² sensitive area. With a threshold energy set at 1 MeV, a neutron detection efficiency of 3.0×10^{-4} cps/nv was obtained for a ^{252}Cf source. The combination of a radiation-resistant front-end integrated circuit and a diamond detector resulted in an estimated γ-ray noise level of 0.001 cps at 0.915 MeV, based on the measurements with γ-rays at a dose rate of up to 600 Gy/h using a ^{60}Co source. Furthermore, at a dose rate of 1 kGy/h, the γ-ray noise was 0.0004 cps, satisfying the S/N ratio of ≥1 required by the Feynman-α method. We suggest that by using 1024 diamonds in the future, the criticality proximity monitoring system could achieve a neutron detection efficiency of 1.9 cps/nv.

*Corresponding author: e-mail: odahokudaikengo64@eis.hokudai.ac.jp
https://doi.org/10.18494/SAM5597

ISSN 0914-4935
https://myukk.org/

1. Introduction

In the process of removing fuel debris from the Fukushima Daiichi Nuclear Power Plant, it is essential to establish a criticality management method that prevents criticality caused by changes in the shape of the fuel debris and the amount of water, as well as excessive radiation exposure to the general public and workers in the event of criticality. To address this issue, the International Research Institute for Nuclear Decommissioning (IRID) is promoting the development of fuel debris criticality control technology, led by reactor plant manufacturers.(1) One of the major challenges identified in this effort is the development of a lightweight criticality proximity monitoring system with a neutron detection sensitivity of several cps/nv, capable of measuring weak neutrons from fuel debris in an environment with a high γ-ray dose rate of up to 1 kGy/h.(2)

The criticality proximity monitoring system used in the initial stages of debris removal needs to be inserted into the primary containment vessel through a narrow penetration. There are strict weight restrictions on the payload of the fuel debris removal device, and the improved device for the initial removal is planned to weigh 50 kg.(3) In addition, a neutron detection sensitivity of several cps/nv is required to meet the requirements of the reactor noise analysis method.

In the future, to investigate the condition of the fuel debris remaining inside the reactor pressure vessel, it will also be necessary to use a neutron detector of the same type that can be inserted into a dry tube. Generally, a fission ionization chamber is used as a neutron detector in such environment with a high γ-ray dose rate. However, to achieve sufficient detection sensitivity, the detector must be made larger. Furthermore, obtaining permission to use a fission ionization chamber containing nuclear fuel material in a damaged reactor is expected to be highly challenging. Therefore, an alternative solution is needed.

At IRID, the following are being evaluated: (a) neutron gas detectors, including an improved ^{10}B proportional counter and a corona detector, and (b) a SiC semiconductor neutron detector. Regarding the former, it has been estimated that, a ^{10}B proportional counter (neutron detection sensitivity: 2 cps/nv), which can be used to evaluate criticality by the Feynman-α method within a one-hour measurement, would require a lead shielding thickness of 2 cm. However, its total weight would exceed 150 kg.(1) The latter is currently under development and is assumed to operate at 100 Gy/h from the perspective of the signal-to-noise ratio with γ-rays and circuit noise.(3) However, it is not designed to withstand 1 kGy/h. Additionally, the electronic components of the data transfer circuit require tungsten shielding to ensure radiation resistance.

To address the above-mentioned issues, we are developing the criticality proximity monitoring system that is expected to have high radiation resistance and low sensitivity to γ-rays, as shown in Fig. 1. This device consists of a neutron detector composed of diamond detector elements and neutron-to-charged-particle converters, as well as radiation-resistant silicon semiconductor integrated devices(4,5) that have been developed through high-energy accelerator experiments.

To achieve the required performance of a maximum permissible operating γ-ray dose rate of 1 kGy/h or more, the diamond membrane underwent further processing, and the electrode structure was improved. Furthermore, the response of these diamond detector elements in combination with a new measurement circuit to γ-ray dose rates of up to 1.5 kGy/h was

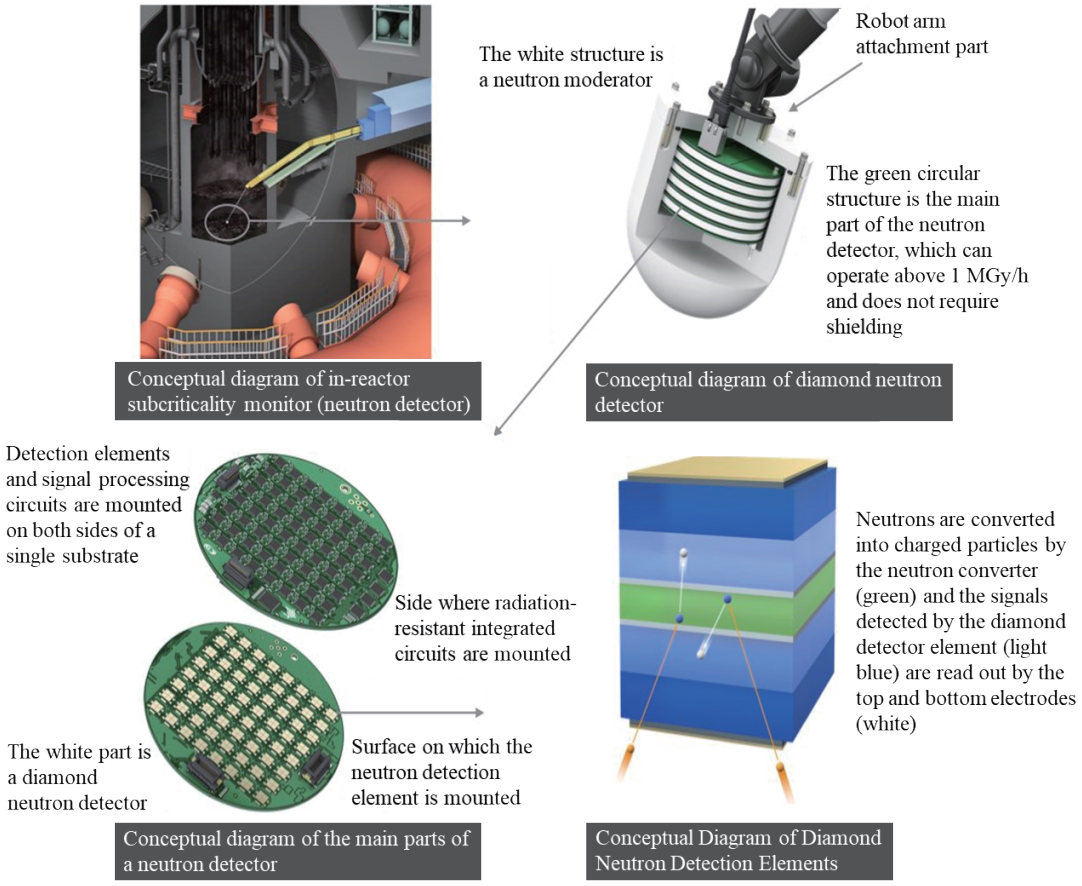

Fig. 1. (Color online) Image of actual criticality proximity monitoring system under development.

evaluated. Additionally, the neutron sensitivity of the system after integrating a ^{6}LiF neutron-to-charged-particle converter with diamond detector elements was measured, and then the neutron detection efficiency of the entire system was estimated.

2. Experimental Procedure

2.1 Growth of single-crystal diamond membranes and fabrication of radiation detectors

In this study, seven diamond detectors were fabricated using single-crystal diamond membranes grown at Hokkaido University and an electronics-grade single-crystal diamond membrane grown by Element Six Ltd., as shown in Table 1.

The following is an outline of the method used to grow the diamonds at Hokkaido University.[6] Homoepitaxial diamond layers were grown by the CVD method[7] on high-pressure and high-temperature (HP/HT) type IIa single-crystal diamond substrates[8] from Sumitomo Electric Industries, with the (001) plane tilted 3 degrees in the <110> direction. To obtain freestanding diamond membranes by the lift-off method,[9] ion implantation layers were

Table 1
List of detectors fabricated (Detectors #4–7 were made by dividing a 9-mm-square diamond membrane grown at Hokkaido University into four parts).

ID	Producer	Thickness	Processing	Detector Structure
Detector #1	HU	66 μm	–	Al/diamond/TiC/Au
Detector #2	HU	46 μm	–	Al/diamond/TiC/Au
Detector #3	E6	50 μm	–	Al/diamond/TiC/Au
Detector #4	HU	80 μm	–	Al/diamond/TiC/Au
Detector #5	HU	70 μm	IBE 10 μm	Al/diamond/TiC/Au
Detector #6	HU	60 μm	IBE 20 μm	Al/diamond/TiC/Au
Detector #7	HU	72 μm	IBE 10 μm, p+ diamond	Al/diamond/p+ diamond/TiC/Au

IBE: Ion Beam Etching, HU: Hokkaido University, E6: Element Six Ltd.

formed on the diamond substrates beforehand. The typical synthesis conditions were a $CH_4/(H_2+CH_4)$ ratio of 0.2%, a gas pressure of 110 Torr, a substrate temperature of 900 ℃, a microwave plasma power of 700–1100 W, and a growth rate of 0.48 μm/h. The CVD-grown layers were then separated by electrochemical etching to obtain freestanding diamond membranes.

The detector structure consisted of a simple electrode–diamond–electrode configuration, with an Al Schottky electrode and a TiC/Au ohmic electrode. The Al electrode was deposited by the resistive heating evaporation method, whereas the Ti/Au electrode was deposited by the electron beam evaporation method. After Ti deposition, the TiC layer was formed by annealing at 400 ℃ for 30 min, followed by Au deposition by the resistive heating evaporation method. The diamond membrane with electrodes was placed in an Al detector enclosure. The TiC/Au electrode was connected to the SMA receptacle, and the Al electrode was connected to the ground of the detector enclosure.

Detectors #1 and 2 were made of single-crystal diamond membranes grown at Hokkaido University with the structure described above. Detector #3 was made of an electronics-grade single-crystal diamond[10] membrane grown by Element Six Ltd. with a thickness of 50 μm, using the same process and structure as Detectors #1 and 2.

Detectors #4 to 7 were fabricated to confirm the effects of etching and a p+ diamond layer, which are intended to reduce charge-up due to γ-rays. To minimize the effect of the diamond material used, four detectors were fabricated by laser cutting a 9-mm-square single-crystal diamond membrane with a thickness of 80 μm, as shown in Fig. 2(a). Detector #4 has the same structure as Detectors #1–3. Diamond membranes fabricated by the lift-off method at Hokkaido University have empirically shown that the defects and impurities on the lift-off separation surface (early growth layer) are higher than those on the growth surface (late growth layer). Therefore, Detectors #5 and 6 were each etched by 10 and 20 μm, respectively, using ion beam etching (IBE) on the lift-off separation surface. TiC/Au electrodes were then formed, followed by the formation of Al electrodes on the opposite surface. For detector #7, the lift-off separation surface was etched by 10 μm using IBE, followed by the deposition of a 2 μm boron-doped p+ diamond layer by the CVD method,[11] and then a TiC/Au electrode was formed. In this case, there was unfavorable growth of the boron-doped p+ diamond layer on the opposite surface, so the opposite p+ diamond layer was removed using IBE, and an Al Schottky electrode was

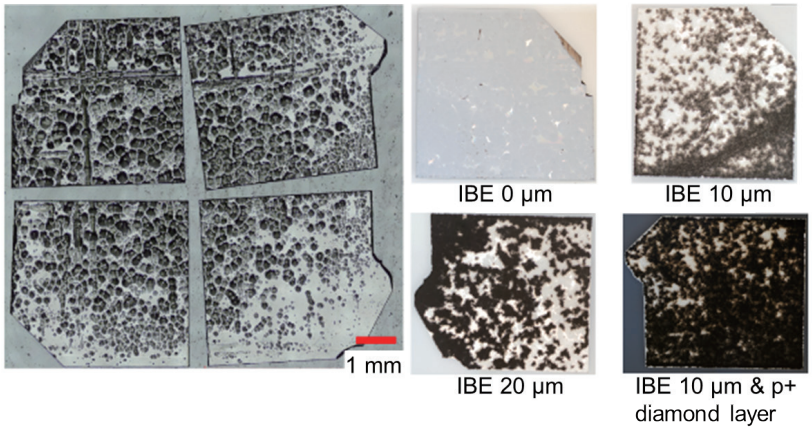

Fig. 2. (Color online) Optical microscopy images of (a) 9-mm-square diamond membrane (growth surface) after laser cutting and (b) processed surface (lift-off separation surface) under each condition (IBE 0 μm, IBE 10 μm, IBE 20 μm, and B-doped p+ diamond layer after IBE 10 μm) used for Detectors #4–7.

formed. Figure 2(b) shows optical microscopy images of the lift-off separation surface of the diamond membranes used in each detector. A black pattern was observed in the sample that underwent IBE.

2.2 Evaluation of basic performance of fabricated diamond detectors

The induced charge distribution measurement of the detectors was carried out using 5.486 MeV α-particles from a ^{241}Am source, directed into the Al electrode of the detector in a vacuum at room temperature. The results are summarized in Table 2. A preamplifier (ORTEC 142A), a main amplifier (ORTEC 672), a high-voltage power supply (ORTEC 428), and a multichannel analyzer (WE500) were used for this measurement. The charge collection efficiency (CCE) was derived on the basis of a comparison with a silicon semiconductor detector (CU-1250-100; EG&G ORTEC), and the average electron–hole pair generation energies for silicon and diamond, ε_{Si} = 3.62 eV[12] and $\varepsilon_{Diamond}$ = 13.1 eV,[13] respectively, were adopted. For Detectors #1–7, the applied voltage was ±1 V/μm, and the switching between electrons and holes was measured by reversing the polarity of the applied voltage. Detectors #4–7 were fabricated from a single diamond membrane to eliminate the effect of the diamond material used. However, Fig. 2(a) shows that each has a different surface roughness, with a maximum surface roughness R_a of approximately 10 μm. Although it is possible that changes in the way α-particles enter the diamond due to surface roughness may affect the detector operation, the α-particles are completely absorbed in the diamond even with a surface roughness of 10 μm, considering that the thickness of the diamond substrate is 60–80 μm, and the range of the 5.486 MeV α-particles in the diamond is 14 μm. Therefore, the effect on the detector operation is considered to be negligible. In fact, the differences in the values shown in Table 2 are small.

Table 2
Charge collection efficiency and energy resolution of the diamond detectors.

ID	Charge collection efficiency (%)		Energy resolution (%)	
	Electron	Hole	Electron	Hole
Detector #1	100.5 ± 0.1	99.4 ± 0.1	0.30	0.32
Detector #2	98.4 ± 0.2	99.1 ± 0.2	0.54	0.37
Detector #3	98.3 ± 0.3	97.9 ± 0.1	0.61	0.35
Detector #4	99.8 ± 0.3	99.0 ± 0.2	0.82	0.47
Detector #5	99.5 ± 0.3	98.5 ± 0.2	0.80	0.52
Detector #6	98.6 ± 0.3	97.5 ± 0.2	0.79	0.38
Detector #7	97.6 ± 0.4	97.5 ± 0.2	0.87	0.47

ε_{Si} = 3.62 eV and $\varepsilon_{Diamond}$ = 13.1 eV were used for derivation. For the charge collection efficiency error, the standard deviation of the α-particle peak portion was adopted.

2.3 γ-ray irradiation experiments

The experiments were conducted at the Nagoya University ^{60}Co γ-ray irradiation facility, the Kyushu University ^{60}Co γ-ray irradiation facility, and the Takasaki Institute for Advanced Quantum Science ^{60}Co γ-ray irradiation facility of the National Institutes for Quantum Science and Technology (QST). In the experiments at Nagoya University and Kyushu University, 5.486 MeV α-particles from an ^{241}Am source were irradiated together with γ-rays at room temperature and in air to facilitate the evaluation of the effects of γ-ray irradiation. The distance between the α-particle source and the detector's incident surface during the measurement was 2.2 mm. Using Stopping and Range of Ions in Matter,[14] the energy loss of 5.486 MeV α-particles in 2.2 mm of air was calculated to be approximately 0.198 MeV. On the basis of the above, the horizontal axis of response functions was calibrated by setting the energy of the α-particle peak to 5.288 MeV. For the measurements observing the time variation in the amount of signals induced by the γ-rays, only γ-ray irradiation was performed. The measurements were conducted using general radiation measurement devices used in Sect. 2.2 and a signal processing front-end integrated circuit designed by the High Energy Accelerator Research Organization (KEK). In both cases, the multichannel analyzer ANSeeN ZMCAN-CH04-01 was used. Table 2 shows that the detector performance was better for holes than for electrons, so the applied voltage was set to −1 V/μm.

At Nagoya University and Kyushu University, ionization chamber dosimeters were used to measure γ-ray dose rates at the irradiation position. At QST, the detector was placed at pre-calibrated positions with known γ-ray dose rates. Measurements were performed using a diamond detector in combination with a front-end integrated circuit designed for an integration time of approximately 100 ns, as shown in Fig. 3. This front-end integrated circuit, designed by KEK and fabricated using 65 nm CMOS technology, has radiation resistance exceeding 1 MGy and can process up to 8 input channels.

2.4 Neutron sensitivity measurement experiment

Diamonds do not have direct sensitivity to neutrons, so a ^{6}LiF sintered body made from 95%-enriched ^{6}Li material, i.e., a neutron-to-charged-particle converter, was developed. ^{6}Li

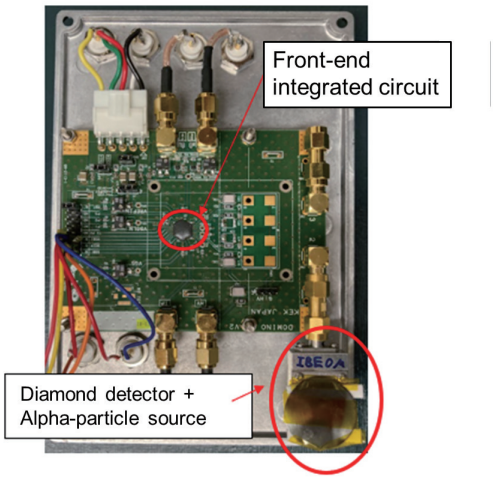

Fig. 3. (Color online) Front-end integrated circuit for signal processing designed by KEK + diamond detector.

captures neutrons and splits into 2.05 MeV $^{4}_{2}$He and 2.73 MeV $^{3}_{1}$T. In this case, $^{4}_{2}$He and $^{3}_{1}$T are considered to fly in opposite directions, approximately 180° apart in accordance with the law of conservation of momentum. Therefore, by placing a ^{6}LiF converter on the detector electrode, it is possible to measure the neutron sensitivity of the diamond, since either charged particle can be detected for each neutron.

The ^{6}LiF was sintered in air at 700 °C for 5 h and then mechanically polished to a thickness of 150–200 μm. Polishing to a thickness of 100 μm or less was likely to cause damage. The above thickness was chosen in consideration of the nuclear reaction cross section of ^{6}Li and the range of the generated charged particles. The use of $^{10}B_4C$ as a neutron-to-charged-particle converter was also considered, but ^{6}LiF was used from the perspective of signal-to-noise ratio.

The ^{6}LiF neutron-to-charged-particle converter was installed on the Al electrode of Detector #2, and the overlapping area between the ^{6}LiF converter and Al electrode was 2.53 mm². The neutron sensitivity of the diamond neutron detector was evaluated in an irradiation field using a ^{252}Cf neutron source, with the neutron flux measured by a calibrated neutron gas detector. The same system and applied voltage as those used in the γ-ray irradiation tests described in Section 2.3 were employed for the measurement.

3. Experimental Results and Discussion

3.1 Assessment of effects of high γ-ray dose rate environments on diamond detectors and attempts to reduce them

Figure 4 shows the γ-ray response functions of Detectors #1 and 3, which were produced using the same process and structure, one from a single-crystal diamond manufactured by Hokkaido University and the other from a single-crystal electronics-grade diamond manufactured by Element Six Ltd.. In the measurement, 5.486 MeV α-particles were

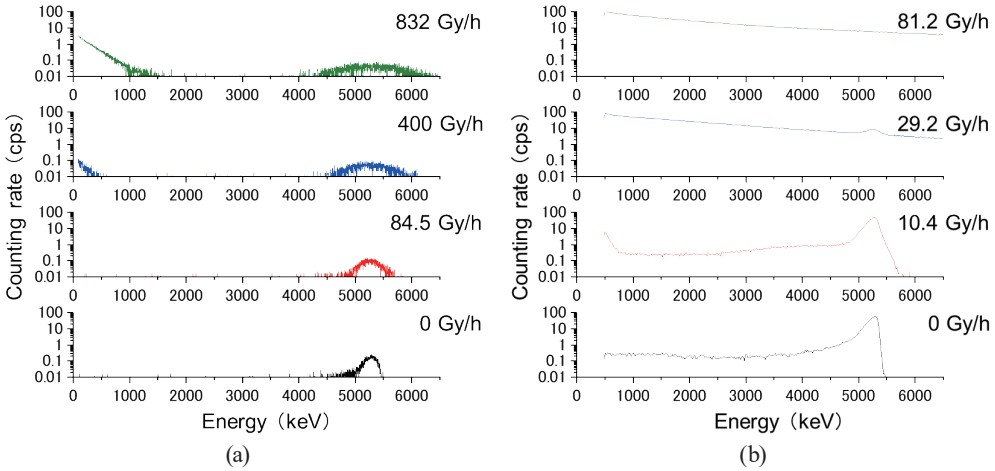

Fig. 4. (Color online) Example of response functions of diamond detectors for α-particles under several γ-ray dose rate in air: (a) Detector #1 made with a diamond grown by Hokkaido University (thickness: 66 μm) and (b) Detector #3 made with a diamond grown by Element Six (thickness: 50 μm).

simultaneously injected in air. The measurements were conducted using general radiation measurement devices.

Detector #1, made from a diamond grown by Hokkaido University, showed almost no signal from γ-rays at a γ-ray dose rate of 84.5 Gy/h. At a γ-ray dose rate of 400 Gy/h, signals from the γ-rays were observed in the low-energy part, and the energy resolution of the α-particles peak deteriorated because the baseline of the preamplifier output fluctuated owing to the influence of the γ-ray. This was largely due to the influence of the integration time of the main amplifier. This measurement was carried out at the Nagoya University ^{60}Co irradiation facility. At the maximum γ-ray dose rate of 832 Gy/h at the facility on the day of the experiment, signals due to the γ-rays were observed up to around 1.5 MeV, and although the energy resolution deteriorated considerably, the peak from α-particles was clearly observed.

On the other hand, for Detector #3, which was made of commercially available diamond crystals, a clear α-particle peak was observed at a γ-ray dose rate of 10.4 Gy/h, but the γ-ray effect was also observed up to several hundred keV. At a γ-ray dose rate of 29.2 Gy/h, the α-particle peak was barely observed, but the count rate increased significantly overall owing to the signals caused by the γ-rays. When the dose rate was increased further to 81.2 Gy/h, the α-particle peak was completely swallowed up by the signal related to the γ-ray and could not be distinguished.

The signals caused by γ-rays are considered to be pseudo-signals that occur when charge is captured in the crystal upon γ-ray irradiation and subsequently released. Although the impurities in the commercially available diamond used for Detector #3 were kept below the detection limit of secondary ion mass spectrometry, luminescence due to structural defects is generally observed in cathodoluminescence measurements. On the other hand, luminescence due to structural defects is negligible in the diamond made by Hokkaido University.[6] Therefore, it is highly likely that the γ-ray effect observed in the commercially available diamond detector is due to charge capture levels caused by structural defects. On the other hand, there are also

reports of detectors made from commercially available diamond crystals operating under a γ-ray dose rate of approximately 100 Gy/h; this may be due to factors such as variations in crystal quality and the effects of machining.

Next, the operational stability of the detectors in a high γ-ray dose rate environment was evaluated. The measurements were conducted using general radiation measurement devices. Figure 5 shows the change over time in the count rate when continuous measurement was performed for one hour in an environment with a γ-ray dose rate of 832 Gy/h for Detectors #1 and 6. The vertical axis shows the number of signals of all energies per second, and the horizontal axis shows the elapsed time. In Detector #1, the counting rate gradually increased from the start of measurement until around 700 s, and then an instantaneous large count rate was recorded. In particular, after 3000 s, the counting rate increased in a spike-like manner and the frequency of spikes increased. In contrast, Detector #6, which had undergone IBE of 20 μm on the lift-off separation surface, had a base count rate of more than 1000 cps, which was five times that of Detector #1. However, there was little change over time, and there was no spike-like increase in the counting rate. The thicknesses of the crystals of these two detectors were almost the same, and the electrode structure and signal readout circuit were completely the same. Therefore, it is considererd that the density of charge capture levels in the diamond crystal exerts an effect on the response to γ-rays. This result indicates that it is important to lower the density of charge capture in the diamond depending on the growth conditions and substrates used. Furthermore, it can be judged that the removal of the lift-off separation surface by IBE was also effective.

To investigate the effect of removing the lift-off separation surface by IBE in more detail, the α-particle spectra of Detectors #4, 5, and 7, which were made from the same single-crystal diamond membrane, were measured in an environment with a γ-ray dose rate of 260 Gy/h. The measurements were conducted using general radiation measurement devices. The results are shown in Fig. 6. As summarized in Table 1, Detectors #4–7 were fabricated by dividing the single-crystal CVD diamond membrane grown on a 9-mm-square HP/HT type IIa single-crystal

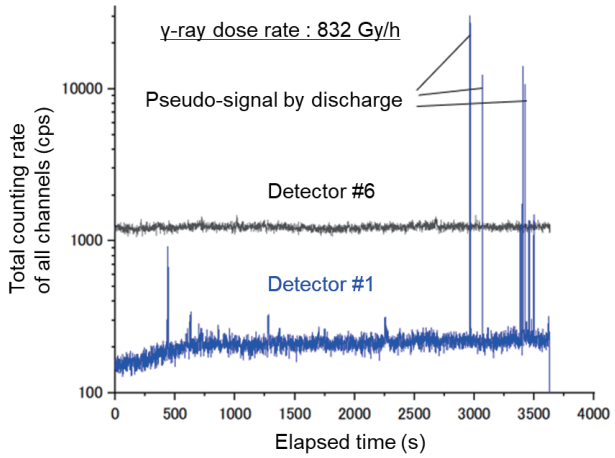

Fig. 5. (Color online) Time-dependent change in the counting rate of Detectors #1 and 6 in an environment with a γ-ray dose rate of 832 Gy/h. The thicknesses of Detectors #1 and 6 were 66 μm and 60 μm, respectively. The lift-off separation surface of Detector #6 was removed by IBE to a depth of 20 μm.

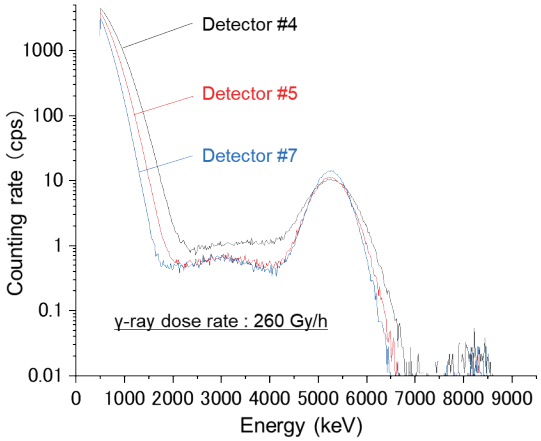

Fig. 6. (Color online) Example of 5.486 MeV α-particle response function in a 260 Gy/h γ-ray dose rate environment for detectors made from the same diamond membrane (Detector #4: no IBE, Detector #5: IBE 10 μm, Detector #7: IBE 10 μm & p+ diamond layer).

diamond substrate into four equal parts. Detector #4 was not subjected to IBE and was used as is. Detector #5 had 10 μm of the lift-off separation surface removed by IBE. Detector #7 was fabricated by first removing 10 μm of the lift-off separation surface by IBE and then synthesizing a p+ diamond layer. This was done to enable the TiC/Au electrode to collect charges more quickly. As seen in Fig. 6, the signals from γ-rays appearing below 2.5 MeV decrease in the order of Detectors #4, #5, and #7. This indicates that IBE and the insertion of the p+ diamond layer are effective in reducing the signals from γ-rays.

From the above results, the removal of the lift-off separation surface by IBE processing and the addition of a p+ diamond layer between the diamond and the electrode are effective in reducing the signal caused by the γ-rays. In addition, the diamond detector with 20 μm removed by IBE performed stably even at 832 Gy/h. As the generation mechanism of signals related to the γ-ray, charge capture and release in the crystal are considered to be the cause of noise signal, so it was also confirmed that reducing the number of defects and amount of impurities originating from the substrate used and the growth conditions is extremely important.

3.2 Evaluation of effect of γ-ray on diamond detector with front-end integrated circuit fabricated by ASIC technique

As an elemental technology for the criticality proximity monitoring system, a γ-ray irradiation experiment for a measurement element that combined a front-end integrated circuit developed at KEK using radiation-resistant Si semiconductor ASIC technology and a diamond detector fabricated at Hokkaido University was conducted. For comparison, the same diamond detector was connected to general radiation measurement devices, such as ORTEC142A and ORTEC428, which were used in the experiment described in Sect. 2.2, and evaluated. Figure 7 shows an example of response functions for 5.486 MeV α-particles using two different circuit systems in an environment with a γ-ray dose rate of 300 Gy/h. The KEK-designed front-end integrated circuit has a short integration time of 0.1 μs to reduce the effect of noise signals from

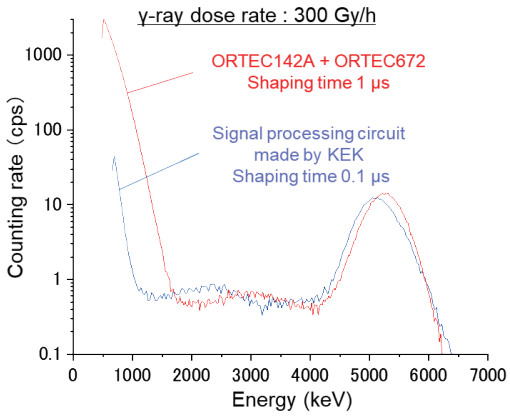

Fig. 7. (Color online) Response functions of the diamond detector for the α-particles when connected to the front-end integrated circuit designed by KEK and general radiation measurement devices (measured at a γ-ray dose rate of 300 Gy/h using Detector #7).

the γ-ray. As a result, it has been successful in reducing the effect of the γ-ray to around 1 MeV. This front-end integrated circuit can handle eight channels of input at once. In an actual criticality proximity monitoring system, four detector elements are fabricated on a 6-mm-square diamond membrane. The neutron-to-charged-particle converters are sandwiched between two diamond membranes, and the signals from the eight detector elements are received by this front-end circuit.

3.3 Evaluation of neutron sensitivity

Figure 8 shows an example of the neutron response function for the diamond neutron detector described in Sect. 2.4. The horizontal axis of the response function was calibrated by setting the high-energy edge to the energy of the triton, 2.73 MeV. The thermal neutron flux of the measurement field constructed with polyethylene blocks was measured using a calibrated ^{6}Li glass scintillator and a $^{10}BF_3$ proportional counter, and the result was 127.5 n/cm^2/s. If the threshold mentioned in Sect. 3.4 was set to 1 MeV and signals with energies above 1 MeV were counted as neutron signals, the detection efficiency of the diamond neutron detector used was 3.2 × 10 cps/nv. Furthermore, when combined with the front-end circuit module shown in Fig. 3, the neutron detection efficiency was 3.0×10^{-4} cps/nv. To obtain a more accurate detection efficiency for the prototype diamond neutron detector, it was evaluated using the ^{252}Cf neutron source at the Radiation Standards Facility of the Japan Atomic Energy Agency, and a thermal neutron detection efficiency of 3.7×10^{-4} cps/nv was obtained.

3.4 Evaluation of noise signals caused by γ-ray at dose rate of 1 kGy/h

To ensure a sufficient signal-to-noise ratio (neutron signal/noise signal due to γ-ray) in an actual criticality proximity monitoring system, we have been working towards setting the energy threshold for discriminating between γ-ray and neutrons at 1 MeV, through measures such as reducing the noise signal caused by the γ-ray and selecting neutron-to-charged-particle

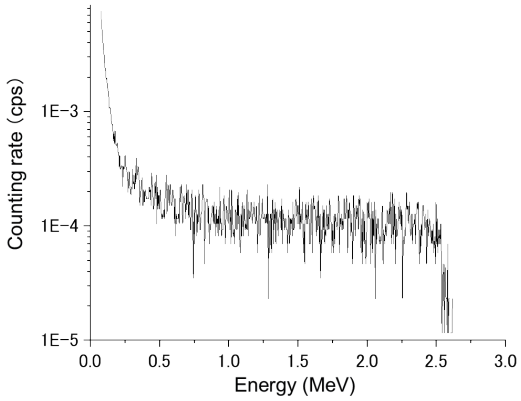

Fig. 8. (Color online) An example of response function of the diamond neutron detector for neutrons from a ^{252}Cf source.

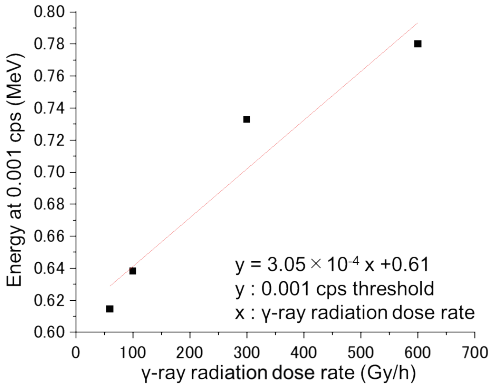

Fig. 9. (Color online) Dose rate dependence of the energy at which the noise signal counting rate caused by the γ-ray reaches 0.001 cps using Detector #2 and KEK-designed front-end integrated circuit (by extrapolation, the energy at which the count rate reaches 0.001 cps at 1 kGy/h was estimated to be 0.915 MeV).

converters. In the Feynman-α method, which is a typical method for evaluating criticality proximity, it is said that the prompt neutron decay constant α can be measured if the neutron counting rate/counting rate of noise signal caused by γ-ray is ≥ 1. To satisfy this condition, the counting rate of noise signals caused by the γ-ray of 0.001 cps at a γ-ray dose rate of 1 kGy/h must be lower than 1 MeV.

This evaluation was carried out at the Kyushu University ^{60}Co irradiation facility and the QST Takasaki Institute ^{60}Co irradiation facility. Detector #2 and the KEK-designed front-end integrated circuit module shown in Fig. 3 were used in the measurement.

At the Kyushu University ^{60}Co irradiation facility, noise signals were evaluated at dose rates up to 600 Gy/h on the day of the experiment. In Fig. 9, the energy corresponding to 0.001 cps is plotted on the vertical axis, whereas the γ-ray dose rate is plotted on the horizontal axis. By extrapolating these results, the energy corresponding to 0.001 cps at 1 kGy/h was determined to be 0.915 MeV. The threshold of 1 MeV was met, ensuring neutron detection sensitivity.

To confirm more directly that the count rate of the noise signal caused by the γ-ray is less than 1 MeV at 1 kGy/h, an experiment using the same detector and circuit at the ^{60}Co irradiation facility at the Takasaki Institute of the QST was conducted. The results are shown in Fig. 10. The

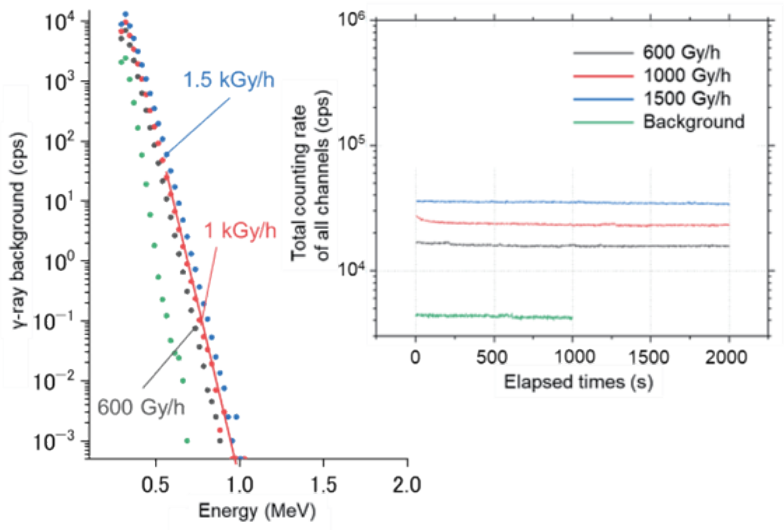

Fig. 10. (Color online) Dose rate dependence of counting rate of noise signal caused by γ-ray using Detector #2 and KEK-designed front-end integrated circuit (directly confirmed to be less than 0.001 cps at 1 kGy/h, and also that the detector works stably at 1.5 kGy/h).

γ-ray counting rate at 1 MeV at 1 kGy/h was 0.0004 cps, directly proving that it is possible to measure neutrons with the desired signal-to-noise ratio. The detector also operated stably at 1.5 kGy/h.

4. Conclusions

In this report, we summarized the development of diamond detectors as part of the development of elemental technologies for the criticality proximity monitoring system used in the decommissioning of the Fukushima Daiichi Nuclear Power Plant. For this monitoring system, the maximum permissible dose rate during operation is 1 kGy/h or more, and because of the payload limitations of the insertion machine, lead shielding cannot be used.

Experiments on γ-ray irradiation of diamond detection elements were conducted; the effectiveness of removing the lift-off separation surface by IBE and introducing a p+ diamond layer as a measure to reduce noise signals caused by the γ-ray was revealed. A prototype of a ^{6}LiF sintered neutron-to-charged-particle converter with a thickness of 180 μm was fabricated. When combined with a diamond detector with a sensitive area of 2.53 mm^2 and a threshold of 1 MeV, a detection efficiency of 3.0×10^{-4} cps/nv was obtained for neutrons from a ^{252}Cf source.

When a radiation-resistant front-end integrated circuit developed by KEK was combined with a diamond detector made by Hokkaido University, the energy of noise signals of 0.001 cps caused by the γ-ray in experiments with a γ-ray dose rate of up to 600 Gy/h was estimated to be 0.915 MeV. Furthermore, the noise signal caused by γ-ray at 1 kGy/h was measured to be 0.0004 cps, and it was demonstrated that the S/N ratio of ≥1 required by the Feynman-α method can be secured at 1 kGy/h. From the above results, it was clarified that if 1024 diamonds are used in the criticality proximity monitoring system to be developed in the future, a neutron detection efficiency of 1.9 cps/nv can be expected.

To realize a system using 1024 diamond detector elements with a 6 mm square size, mass production technology for detector diamond membranes is essential. Currently, Hokkaido University is capable of producing 16 detector diamond membranes in a single synthesis, but for further mass production, it is necessary to increase the synthesis area and improve the growth rate to shorten the synthesis time. Additionally, owing to factors such as capacitance, the diamond substrates need to be thinned to around 50 μm, making them prone to breakage during the detector element manufacturing process, which results in lower yield. Therefore, developing a manufacturing process that ensures high yield is also important. Furthermore, in the current signal processing front-end circuit, variations in the characteristics of each detector element are manually adjusted, but KEK is also developing an automatic adjustment function to accommodate the increase in the number of detector elements. In the future, it will be necessary to combine these detector elements with the signal processing front-end circuit and demonstrate the capability of neutron measurement in high gamma-ray environments.

Acknowledgments

This work was supported by JAEA Nuclear Energy S&T and Human Resource Development Project through concentrating wisdom Grant Numbers JPJA20P20336542 and JPJA23P23813844.

References

1 FY 2017 Supplementary Budget, "Decommissioning and Contaminated Water Countermeasures Project Fund", Advancement of Methods and Systems for Retrieving Fuel Debris and Internal Contaminated Structures (Technical Development for Establishing Criticality Control Methods), Final Report for the FY 2018 Implementation: https://irid.or.jp/_pdf/20180000_04.pdf (accessed March 2025) (in Japanese).
2 K. Okumura, E. S. Riyana, W. Sato, H. Maeda, J. Katakura, S. Kamada, M. J. Joyce, and B. Lennox: Prog. Nucl. Sci. Technol. **6** (2019) 108. https://doi.org/10.15669/pnst.6.108
3 FY 2016 Supplementary Budget, "Decommissioning and Contaminated Water Countermeasures Project Fund", Advancement of Basic Technology for Retrieval of Fuel Debris and Internal Structures of the Reactor, Final Report for the FY 2017 Implementation: https://irid.or.jp/wp-content/uploads/2018/06/20170000_09.pdf (accessed March 2025) (in Japanese).
4 T. Kishishita, G. Sato, H. Ikeda, M. Kokubun, T. Takahashi, T. Idehara, H. Tsunemi, and Y. Arai: Nucl. Instrum. Methods Phys. Res., Sect. A, **636** (2011) S143. https://doi.org/10.1016/j.nima.2010.04.099
5 Y. Sato, Y. Fujita, E. Hamada, T. Kishishita, T. Mibe, O. Sasaki, M. Shoji, T. Suehara, M. Tanaka, J. Tojo, T. Tsutsumi, T. Yamanaka, and T. Yoshioka: Nucl. Instrum. Methods Phys. Res., Sect. A, **969** (2020) 164035. https://doi.org/10.1016/j.nima.2020.164035
6 T. Shimaoka, J. H. Kaneko, M. Tsubota, H. Shimmyo, H. Watanabe, A. Chayahara, H. Umezawa, and S. Shikata: Europhys. Lett., **113** (2016) 62001. https://doi.org/10.1209/0295-5075/113/62001
7 M. Kamo, Y. Sato, S. Matsumoto, and N. Setaka: J. Cryst. Growth, **62** (1983) 642. https://doi.org/10.1016/0022-0248(83)90411-6
8 H. Sumiya, N. Toda, and S. Satoh: New Diamond Front. Carbon Technol. **10** (2000) 233. https://www.webofscience.com/wos/woscc/full-record/WOS:000165889400002
9 Y. Mokuno, A. Chayahara, and H. Yamada: Diamond Relat. Mater., **17** (2008) 415. https://doi.org/10.1016/j.diamond.2007.12.058
10 H. Pernegger, S. Roe, P. Weilhammer, V. Eremin, H. Frais-Kölbl, E. Griesmayer, H. Kagan, S. Schnetzer, R. Stone, W. Trischuk, D. Twitchen, and A. Whitehead: J. Appl. Phys., **97** (2005) 073704. https://doi.org/10.1063/1.1863417
11 J. Kaneko, M. Katagiri, Y. Ikeda, and T. Nishitani: Nucl. Instrum. Methods Phys. Res., Sect. A, **422** (1999) 211. https://doi.org/10.1016/S0168-9002(98)01096-1

12 G. F. Knoll: Radiation Detection and Measurement, B. Zobrist, R. Factor, and S. Malinowski Eds. (John Wiley & Sons, Inc., New York, 1989) 3nd ed., Chap. 11.
13 S. F. Kozlov, R. Stuck, M. Hage-Ali, and P. Siffert: IEEE Trans. Nucl. Sci. NS-**22** (1975) 160. https://doi.org/10.1109/TNS.1975.4327634
14 J. Ziegler - SRIM & TRIM: http://www.srim.org (accessed March 2025).